



ELSEVIER

Sedimentary Geology 116 (1998) 13–24

**Sedimentary
Geology**

ExpresSed

Low limit of Mn^{2+} -activated cathodoluminescence of calcite: state of the art

Dirk Habermann, Rolf D. Neuser, Detlev K. Richter *

Department of Geology, Ruhr-University-Bochum, D-44780 Bochum, Germany

Received 23 July 1997; accepted 16 October 1997

Abstract

In the literature, the lower limit for Mn^{2+} -activated cathodoluminescence (CL) of calcite is variously reputed to over a very wide range of values above 10 ppm Mn. Our spectroscopic investigations of the CL response in natural calcite reveal that below 10 ppm manganese content Mn^{2+} -activation is also present. Using the Quantitative High Resolution Spectral analysis of CL (QHRS-CL) an activation by Mn^{2+} in the range of 700 ppb is proved, which cannot be determined visually. So, if not quenched, the minimum Mn^{2+} content for Mn^{2+} -activation is one atom in the irradiated calcite crystal lattice volume. As the intrinsic (background blue) luminescence is used to determine non-altered biogenic calcite, the limit of Mn^{2+} -activation plays an important role in the interpretation of diagenetic processes. Our results of spectroscopic analyses require a revision of current opinions about the diagenesis of calcite as revealed by CL investigation. © 1998 Elsevier Science B.V. All rights reserved.

Keywords: cathodoluminescence; spectral analysis; manganese concentration; intrinsic luminescence

1. Introduction

It is a known fact that cathodoluminescence (CL) of natural calcite is predominantly controlled by the activator and quencher elements Mn^{2+} and Fe^{2+} . Additional activator elements like trivalent REE (Pr, Eu, Sm, Dy, Tb etc.) are also common (Machel et al., 1991; Habermann et al., 1996a).

In pure calcite or with minor traces of substituting elements the intrinsic luminescence (e.g. Sippel and Glover, 1965; Richter and Zinkernagel, 1981; Amieux, 1982; Mason, 1987; Machel et al., 1991) is characterized by a faint blue colour caused by crystal imperfection.

The lower limit of Mn^{2+} -activation has been controversially discussed in the past and there is some disagreement about the visible detection limits of Mn^{2+} -activation. The data range between 10–20 ppm (Ten Have and Heijnen, 1985; Mason and Mariano, 1990; Bruhn, 1995) and 20–1000 ppm (summary in Füchtbauer and Richter, 1988; Machel et al., 1991). Some authors (e.g. Bruhn, 1995; Savard et al., 1995) interpret the visible detection limit of Mn^{2+} -activated CL as a concentration level, below which Mn^{2+} -activation does not occur. However, this interpretation is obviously not consistent with the physics and the theory of luminescence, and seems to be an over-interpretation of the results of visible CL-intensity determination. Other authors (e.g. Walker et al., 1989) point out that there is no reason for Mn^{2+} -activation not to occur at values below

* Corresponding author.

E-mail: dirk.e.habermann@ruhr-uni-bochum.de

15–30 ppm Mn content if the detection system is sensitive and the iron concentration is low.

In general, luminescence intensity is not only controlled by the absolute activator concentration, but also by different kinds of quenching and sensitizing effects. The Mn²⁺-activated CL, however, is controlled by the absolute Mn and Fe concentration (e.g. Habermann, 1997).

Sometimes carbonates without any visible luminescence are termed as 'not activated' (e.g. Bruhn, 1995; Savard et al., 1995). As this is described for pure calcite or calcite with minor traces of substituting elements, this is in fact the intrinsic CL emitted at a relatively low beam energy. In such cases the intrinsic CL could not be visually detected, which does not necessarily imply its absence. Here, HRS-CL spectroscopy (Habermann et al., 1996a) is able to determine the intrinsic CL clearly. The intrinsic luminescence in calcite is often used to determine unaltered biogenic calcite (Qing and Veizer, 1994; Land, 1995). Not only for this reason the beginning of visible luminescence in calcite caused by traces of substituting elements is of special significance.

2. Methods

Our cathodoluminescence examinations were carried out with the 'hot cathode' CL microscope (type HC1-LM) developed at the Ruhr-University Bochum (Neuser, 1995).

The acceleration voltage of the electron beam was 14 keV and the beam current was set to a level gaining a current density of $\sim 9 \mu\text{A}/\text{mm}^2$ on the sample surface. To keep the current density comparable, the stimulation was controlled by the spectrometric analysis of the CL intensity using a hydrothermal calcite from Iceland (sample I-SPAT) as an external standard. The maximum deviation was below $\pm 2\%$ of that standard CL intensity.

Luminescence spectra were obtained by using an EG&G digital triple grating spectrograph with a LN₂-cooled CCD camera attached to the CL microscope by a quartz light guide of 1.5 m in length (Neuser et al., 1996). The CCD camera was cooled down to $-120^\circ\text{C} \pm 0.1^\circ\text{C}$ to get a high signal/noise ratio. Spectra were accumulated within an exposure time of 30 s. For a high lateral resolution the analyzed area was focused to a spot of 30 μm in diameter.

The digital spectra were stored on a computer for further processing using a non-commercial software for *Quantitative High Resolution Spectral analysis of CL emission* (QHRS-CL) developed by the author D.H. This method is the combination of HRS-CL (Habermann et al., 1996a) and a computer-based quantitative CL spectral analysis. The QHRS-CL is calibrated by using PIXE (*Proton Induced X-ray Emission*) for sedimentary, hydrothermal and biogenic calcite in the range of 10 (detection limit of PIXE — Bruhn, 1995) to ~ 4000 ppm Mn and Fe concentrations below ~ 3000 ppm and an empirical error of $\sim 15\%$. By using QHRS-CL, a quantitative proof of Mn below 10 ppm is possible. The relationship between Mn content analyzed by PIXE and Mn²⁺-activated CL intensity is linear between 10 and ~ 1000 ppm provided that in such low concentrations a self-quenching is not efficient. To estimate Mn concentrations below 10 ppm the linear relationship is extrapolated to values below 10 ppm Mn (Fig. 1). In order to compare the QHRS-CL detection limits with those of PIXE, the same criterion for distinguishing a peak from background is applied (Johansson and Campbell, 1988; Homman et al., 1994). The minimum acceptable CL peak area is assumed to be $\sqrt[3]{N_b}$ (N_b is the amplitude of the background at the peak). The calculated detection limit is 0.1–0.2 ppm for QHRS-CL.

Microprobe analyses were done using PIXE at the Ruhr-University Bochum (method in Meijer et al., 1994). Here at an average spot size of 10 μm and a proton energy of 3 MeV, the detection limit for Mn is 10 ppm (Bruhn, 1995).

3. Experiment results

3.1. Intrinsic spectra of calcite

Researching the intrinsic phenomena of carbonates document that the CL emission spectra are marked by five broad bands within the range of 400 to 700 nm. Significant emission maxima are at ~ 400 nm, 575 nm and 640–660 nm (not due to Mn²⁺!) and minor bands at 450 nm and 520 nm. There are several reasons for the shape of the intrinsic CL of carbonates. For example, the recombination of electrons of a Ca⁺–CO₃[–]-centre is a possible reason for the intrinsic blue 420 emission band in calcite

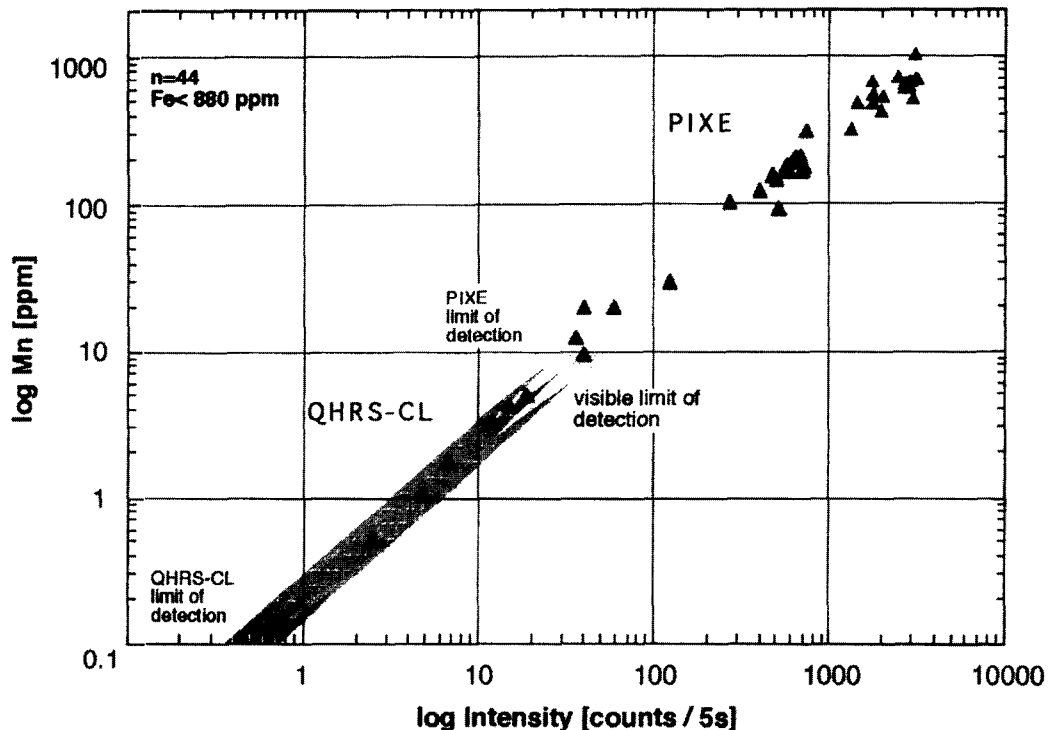


Fig. 1. Correlation between CL intensity (normalized to counts/5 s) and Mn concentration (ppm). The data of PIXE and the high-resolution CL spectroscopy reveal a linear correlation between CL intensity and Mn content above 10 ppm Mn. Below this concentration Mn can be analyzed by QHRS-CL only.

(Calderón et al., 1984). On the other hand the 575 to 640 nm bands seem to be attributed to lattice defects generated by radiation damage, growth defects, or by the electron bombardment. If pure calcite is bombarded by accelerated electrons (15 min and beam density of $\sim 9 \mu\text{A}/\text{mm}^2$), it is remarkable that the intrinsic emission at 575 to 640 nm shows an increase in intensity at a final state of prolonged electron bombardment. However, the level of the 400–450 emission is constant (Fig. 2). The increase of the 574 nm and 640 nm bands could be attributed to the generation of new defects (e.g. broken bondings between the Ca ion and the oxygen ions and also oxygen vacancies). The 575–640 nm bands may be the result of excitement and recombination of unpaired electrons of such defect centres.

The intrinsic portion of the calcite spectrum is characteristic in any case, even with Mn^{2+} and REE activation (Habermann et al., 1996a). If sufficient Fe^{2+} is present, an efficient quenching at ~ 420 nm and 520 nm up to 700 nm is observed.

3.2. Detection and quantitative analysis of low Mn concentration

Our investigations focus on sedimentary, hydrothermal and sinter calcite, brachiopod shells and belemnite rostra. In all samples Mn and Fe concentrations are below 1020 ppm and 880 ppm, respectively. The sum of other substituting elements are below 200 ppm except of Sr and Mg (Table 1). So, the extrinsic CL of the analyzed samples could be clearly attributed to the obviously unaffected Mn^{2+} -activation and sensitizing or quenching by other trace elements could be excluded. This is of importance for the determination of the 'pure' correlation between CL intensity and trace element concentration.

Mn^{2+} causes a well known yellow to orange-red CL in calcite, but dull orange and violet CL colours are also common. PIXE and CL-spectroscopy analyses from samples with low trace element concentration document that dull orange and violet CL are due

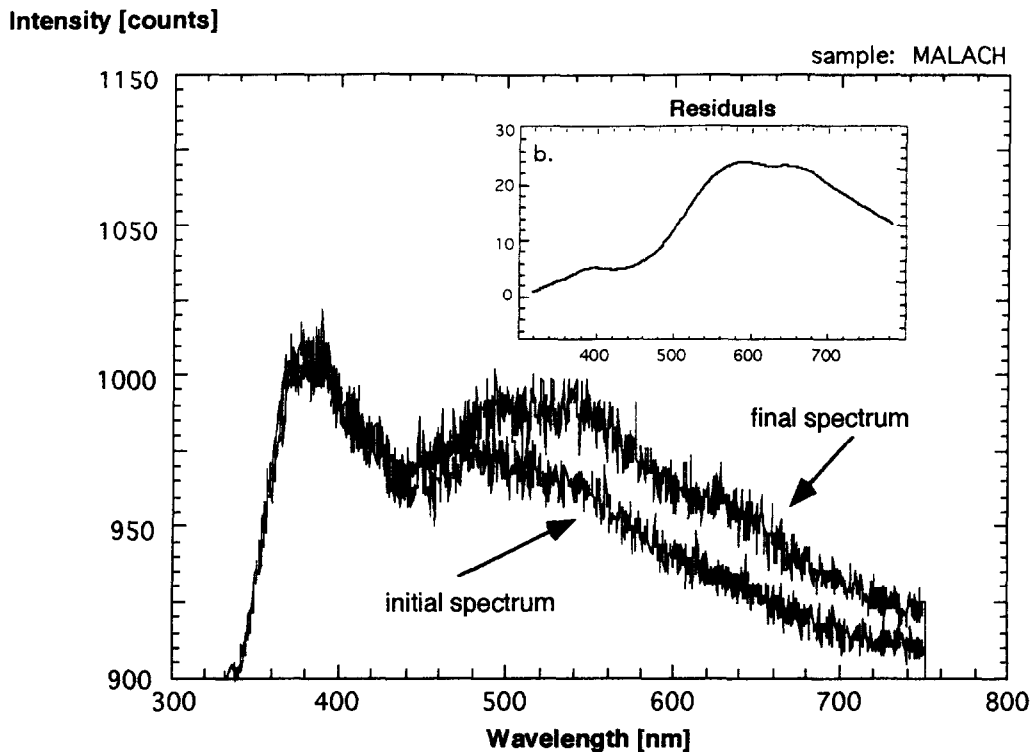


Fig. 2. CL spectra of pure calcite before and after being bombarded by accelerated electrons (15 min and beam density of $\sim 9 \mu\text{A}/\text{mm}^2$). The level of the intrinsic 400–450 emission is constant, where the intrinsic emission at 575 to 640 nm shows an increase in intensity at a final state of prolonged electron bombardment. The increase of the 574-nm and 640-nm bands could be attributed to the generation of new defect centres, e.g. broken bondings between the Ca ion and the oxygen ions.

to Mn below ~ 200 ppm. Calcite with Mn concentrations below 50–60 ppm show only violet to blue CL colours due to the combination of the intrinsic blue and a faint Mn^{2+} -activated orange CL (Fig. 5). There is a continuous transition between blue, violet and orange CL colours in calcite, which is based on the relative and absolute CL intensity of the intrinsic and the Mn^{2+} -activated luminescence. But an objective visual determination of CL intensity — as done in most published studies — is nearly impossible and is scientifically questionable.

The spectroscopically recorded Mn^{2+} -activated CL intensity for Mn concentration in the range of 10 to ~ 1000 ppm documents a linear relationship between CL intensity and Mn content analyzed using a PIXE (Fig. 1).

In some samples a violet luminescence is visible although the Mn concentration is below 10 ppm and below the detection limit of PIXE (Figs. 3 and 5b).

Here, QHRS-CL shows Mn concentrations of ~ 3 ppm and ~ 10 ppm Dy. The latter is also below the detection limit of PIXE and analyzed by QHRS-CL. As the Dy peaks (~ 480 nm, 575 nm and 761 nm) are of low intensity, they do not imply a distinct increase in the CL intensity.

The analyses of blue to blue-violet luminescing zones in a belemnite rostrum (Fig. 5c, sample OP1-19/21) show Mn concentrations of 1 ppm and in a violet zone of the rostrum 19 ppm are detected (Fig. 4a, b).

Investigations of Pleistocene and Recent brachiopod shells reveal that for biogenic calcite intrinsic blue and a Mn^{2+} -activated violet and orange luminescence are characteristic (see also Barbin and Gaspard, 1995). The CL spectrum of the blue-violet zoning of a Pleistocene brachiopod shell shows the typical Mn^{2+} -peak and additional intrinsic background CL peaks (Fig. 4c; see also CL photo in

Table 1
Sample description

No.	Sample	Concentration (ppm)			CL intensity (counts/5 s)	Description	Visible CL colour	Method QHRS-CL*, PIXE**
		Mn	Fe	Sr				
1	K-SUR-P1	12	65	343	36	hydrothermal calcite	v	**
2	K-SUR-P2	20	93	160	40	hydrothermal calcite	v	**
3	DB142-1	3.1	–	50	12.2	hydrothermal calcite	b/v	*/**
4	DB142-2	3.0	–	56	12	hydrothermal calcite	b/v	*/**
5	DB143-P1	98	24	–	273	burial calcite cement	m	**
6	DB143-P4	29	641	79	125	burial calcite cement	d	**
7	SINTER1-2	0.7	NA	NA	2.5	sinter calcite	b	*
8	OPI-19 ^b	19	4	NA	60	calcite: belemnite rostrum	v	**
9	OPI-21 ^b	1	28	NA	5	calcite: belemnite rostrum	b	*/**
10	GAPI-1	4.8	–	–	19	sinter calcite	v	*
11	KAP HIRO1	4	NA	NA	15	Pleistocene brachiopod shell	b/v	*
12	KAP HIRO23	8.2	NA	NA	32	Pleistocene brachiopod shell	v	*
13	MALACH ^a	–	–	557	–	sinter calcite	b	*
14	TREZ-1	1.7	NA	NA	6.7	recent brachiopod shell	b/v	*
15	ISPAT-P1	159	241	661	700	hydrothermal calcite	o	**
16	P2	168	212	674	726	hydrothermal calcite	o	**
17	P3	159	186	637	592	hydrothermal calcite	o	**
18	P4	198	248	476	644	hydrothermal calcite	o	**
19	P5	173	130	362	571	hydrothermal calcite	o	**
20	P6	136	57	389	504	hydrothermal calcite	o	**
21	P7	117	42	307	399	hydrothermal calcite	m	**
22	Fb5 ^b -21	88	845	20	511	burial calcite cement	d/m	**
23	22	64	633	30	578	burial calcite cement	d	**
24	25	400	184	270	1980	burial calcite cement	o	**
25	26	273	172	224	1784	burial calcite cement	o	**
26	27	310	800	130	1331	burial calcite cement	o	**
27	28	465	473	91	1460	burial calcite cement	o	**
28	29	470	488	73	1782	burial calcite cement	o	**
29	30	519	325	45	2006	burial calcite cement	o	**
30	31	669	174	71	3204	burial calcite cement	o	**
31	32	659	207	120	1767	burial calcite cement	o	**
32	33	636	259	128	2668	burial calcite cement	o	**
33	34	590	326	128	2668	burial calcite cement	o	**
34	35	499	540	105	2981	burial calcite cement	o	**
35	36	613	414	74	2865	burial calcite cement	o	**
36	37	696	124	70	2458	burial calcite cement	o	**
37	38	641	98	81	2770	burial calcite cement	o	**
38	39	648	86	91	2934	burial calcite cement	o	**
39	40	668	85	110	3091	burial calcite cement	o	**
40	41	1011	51	84	3054	burial calcite cement	b-o	**
41	TRI-W-1	172	878	133	615	burial calcite cement	o	**
42	2	156	629	169	582	burial calcite cement	o	**
43	3	130	351	167	482	burial calcite cement	m	**
44	4	171	377	249	567	burial calcite cement	o	**
45	5	202	390	116	779	burial calcite cement	o	**

Sr, Fe trace-element analysis and Mn-analysis over 10 ppm were done using PIXE. Mn below the detection limit of PIXE (10 ppm) was done using QHRS-CL and data of this work (NA = not analyzed; – = not detected).

^a Not plotted in Fig. 1.

^b PIXE analysis from Bruhn (1995) (values of sample FB5 are mean of two PIXE analyses).

CL colour description: b = blue; v = violet; d = dull orange; m = moderate orange; o = orange; b-o = bright orange.

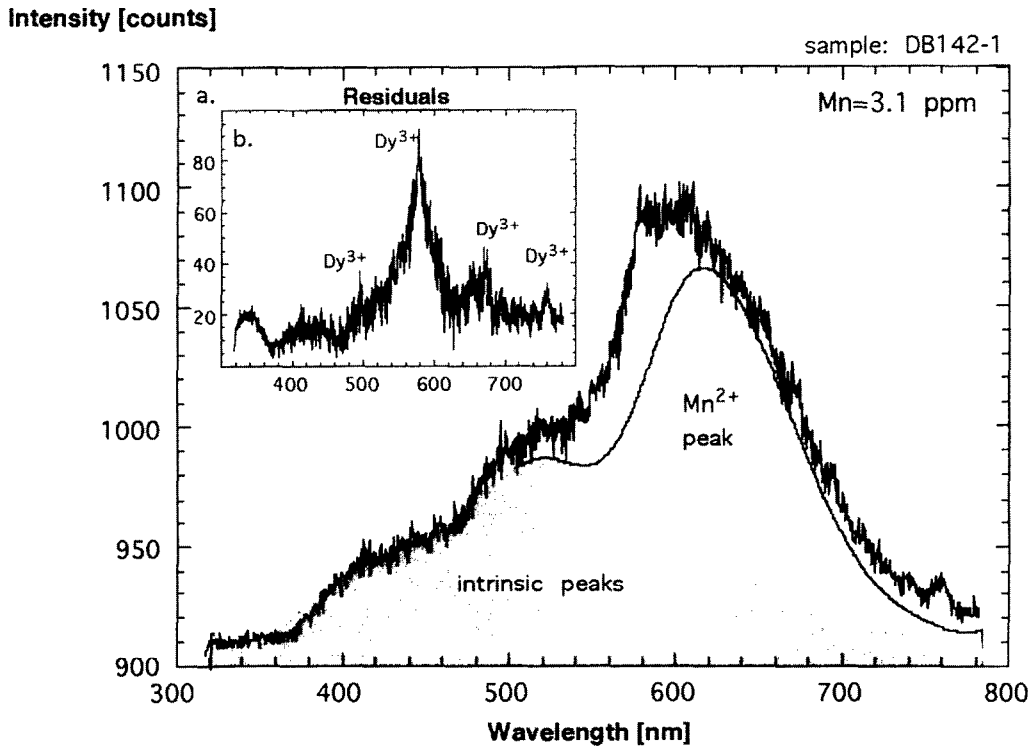


Fig. 3. (a) The Mn concentration of ~ 3 ppm and ~ 10 ppm Dy show intensive peaks. To analyze the CL intensity of Mn and Dy separately, the overlapping of Mn^{2+} -, Dy^{3+} - and intrinsic peaks demanded an exact filtering of the CL spectrum (gray shaded: model spectrum of the Mn^{2+} -peak and the intrinsic peaks). (b) Residuals: the Dy^{3+} -peaks (~ 480 nm, 575 nm and 761 nm) are of low intensity and therefore not effecting a distinct increase in the CL intensity. (Trace element analysis: QHRS-CL; analysis conditions: exposure time 60 s, spot size $30 \mu\text{m}$ diam.)

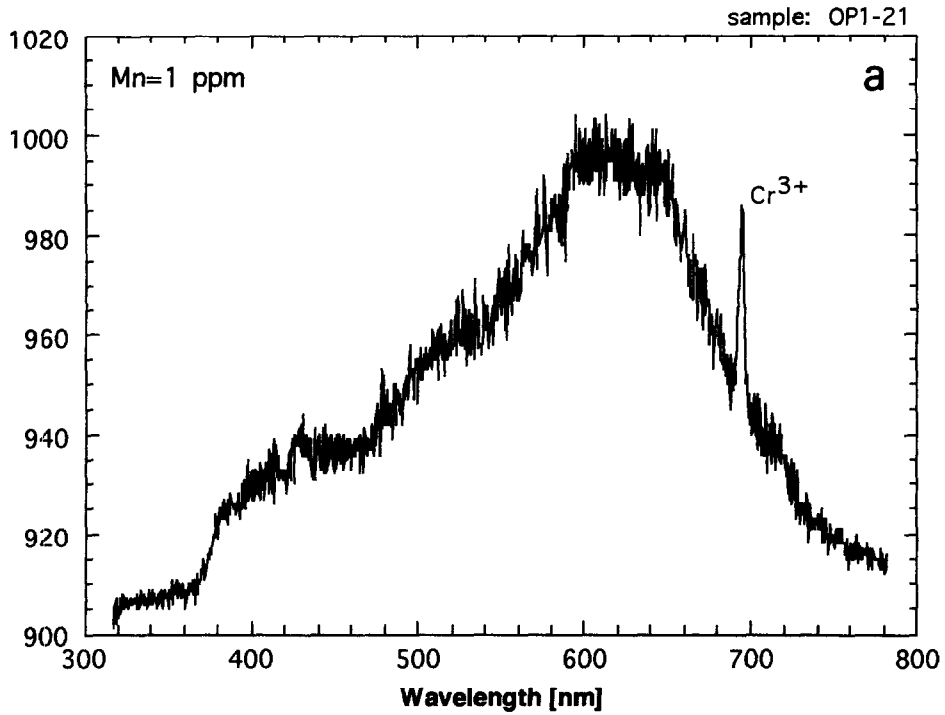
Fig. 5d). In these zones the Mn content is in the range between ~ 4 and 8 ppm. The CL spectra of blue CL zones of recent brachiopod shells (Fig. 4d) also reveal Mn^{2+} -activation below the visible detection limit.

Analyzing very pure natural calcite, our investigations focus on samples of nearly stoichiometric sinter calcite (Fig. 1, sample MALACH) showing a faint blue luminescence. But usually the sinter calcite is characterized by a concentric orange and blue luminescing zonation; here the orange zones are mostly

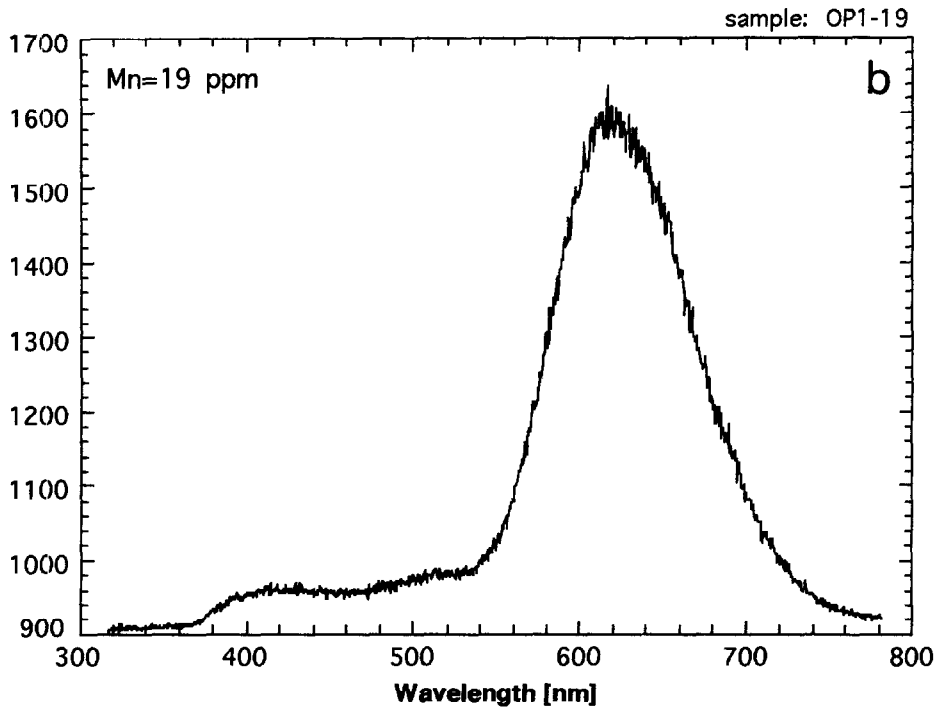
only $1\text{--}50 \mu\text{m}$ in width and attributed to Mn^{2+} . REE (e.g. Sm^{3+} , Pr^{3+} and Dy^{3+}) have been proved too (Habermann et al., 1996a). In addition to the dominant intrinsic bands, the emission spectrum of a blue CL zone shows a subordinate broad band at 605 nm in sinter calcite (Fig. 4e, sample SINTER1-2). This peak is attributed to the Mn^{2+} -activation yielding a Mn concentration of 0.7 ppm (QHRS-CL analysis). The calculated detection limit for this sample is 0.1–0.2 ppm Mn. It has to be mentioned that this is no special case.

Fig. 4. (a) The CL spectrum of a blue luminescing zone in a belemnite rostrum (see Fig. 5c) shows a Mn^{2+} -peak although the Mn content is below 10 ppm. Using QHRS-CL 1 ppm Mn is analyzed for this zone. Cr^{3+} can be analyzed qualitatively too. The latter is uncommon for biogenic unaltered calcite. (Trace element analysis: QHRS-CL; analysis conditions: exposure time 60 s, spot size $30 \mu\text{m}$ diam.) (b) In a violet zone of the rostrum (same sample as (a), see also Fig. 5c) 19 ppm Mn are analyzed using PIXE. Here the Mn^{2+} -peak is much more intense as in the blue zoning. (Trace element analysis: PIXE; CL spectrum: exposure time 60 s, spot size $30 \mu\text{m}$ diam.)

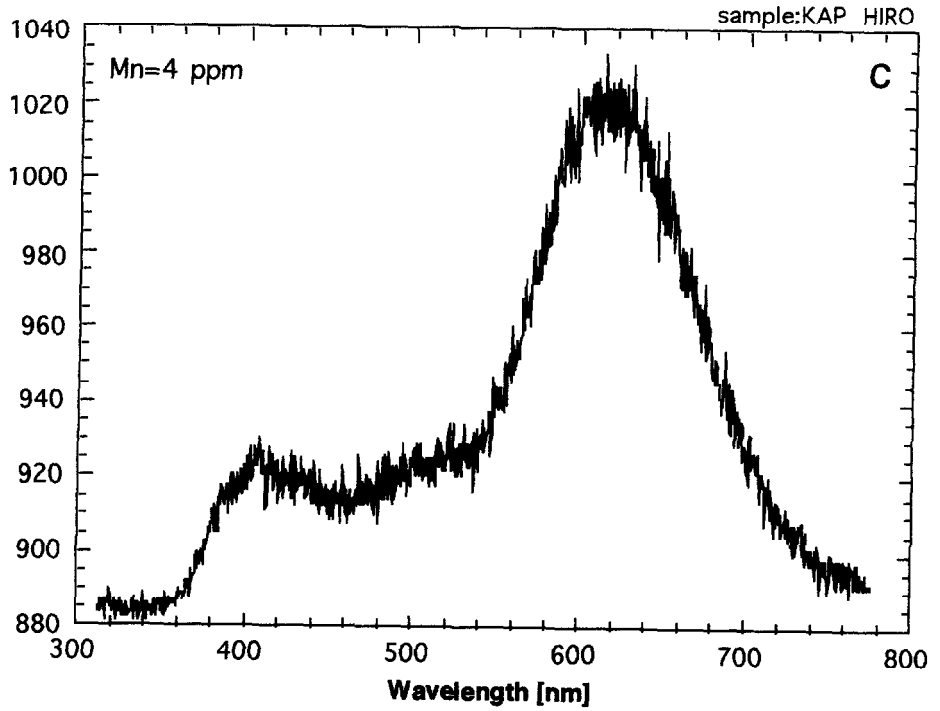
Intensity [counts]



Intensity [counts]



Intensity [counts]



Intensity [counts]

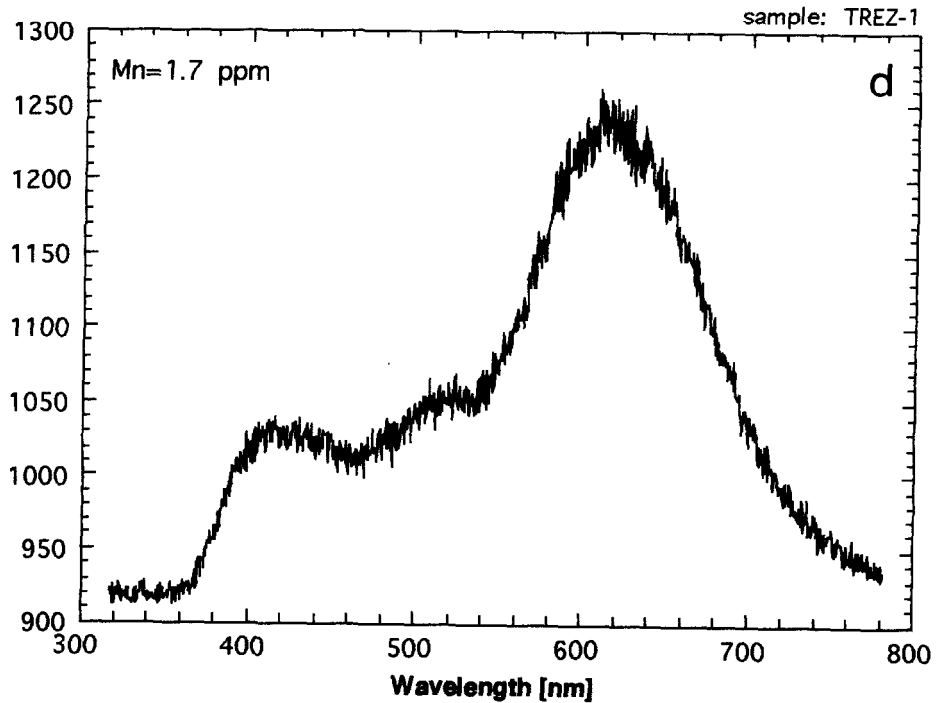


Fig. 4 (continued).

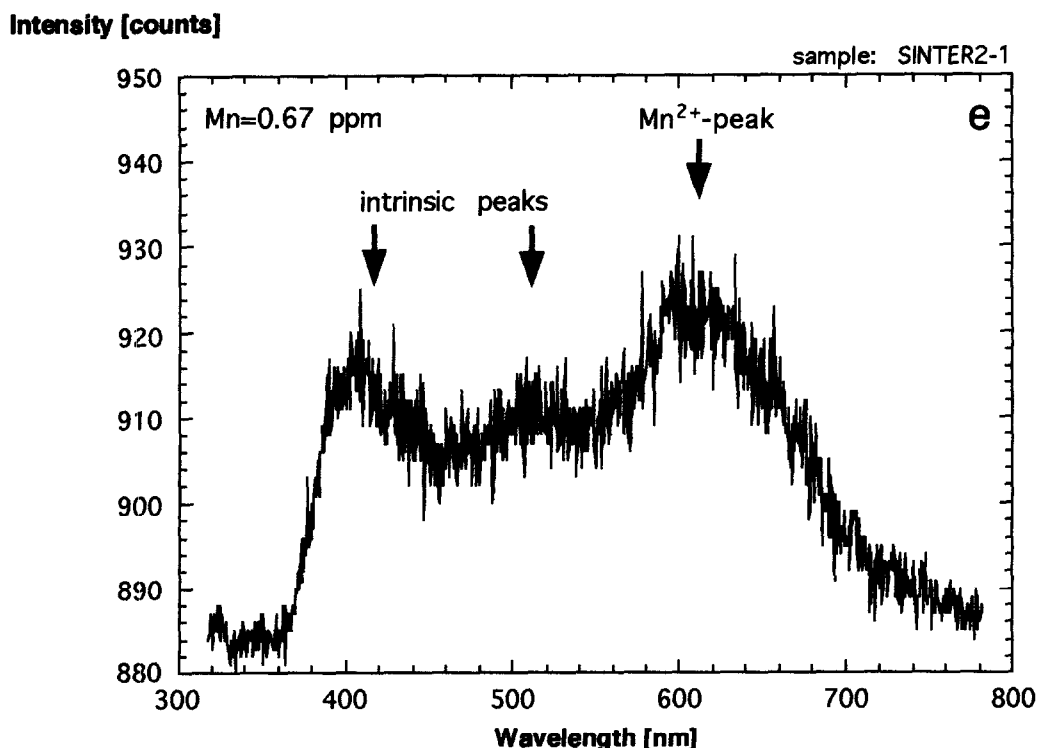


Fig. 4 (continued). (c) Blue-violet zoning is also common in Pleistocene brachiopod shells (see also Fig. 5d). The CL spectrum reveals that this is due to the Mn^{2+} -activation and additional intrinsic CL. The Mn^{2+} -peak intensity is equivalent to 4 ppm Mn. (Trace element analysis: QHRS-CL; analysis conditions QHRS-CL: exposure time 30 s, spot size 30 μm diam.) (d) Blue CL zones of recent brachiopod shells also reveal a Mn^{2+} -activation (1.7 ppm Mn) below the visible detection limit and thus below the PIXE detection limit. (Trace element analysis: QHRS-CL; analysis conditions: exposure time 60 s, spot size 30 μm diam.) (e) The low limit of detection of QHRS-CL is in the range of 0.1–0.2 ppm. Therefore Mn can be analyzed below 1 ppm quantitatively with QHRS-CL. The CL spectrum shows the intrinsic peaks and a Mn^{2+} -peak of low intensity at 605 nm wavelength (the Mn-peak is equivalent to 0.7 ppm Mn). (Trace element analysis: QHRS-CL; analysis conditions: exposure time 60 s, spot size 30 μm diam.)

4. Discussion and conclusions

At the present state QHRS-CL is a powerful technique to determine Mn concentrations from 0.1–0.2 ppm up to 3000 ppm. The optimum range of this method is below 1000 ppm Mn and it still works very efficiently below 200 ppm (Habermann et al., 1996b). Only Mn incorporated in the lattice can be analyzed. There is no open question if small amounts of trace elements are incorporated or not, which is in contrast to other microprobe analysis methods. But in the case of calcite the Mn concentrations analyzed by, for example, PIXE or related methods, will be still in the range of incorporated Mn in the crystal lattice. In the case of some other minerals (e.g. feldspar) the incorporated Fe^{3+} concentration has

not to be in conformity with the analyzed concentration as determined by conventional microprobes (e.g. PIXE, SIMS, EMP).

As the Mn^{2+} -activated CL at about 4 ppm Mn is faintly visible using a 'hot cathode' CL microscope, the lower limit of visible Mn^{2+} -activated CL must be in that range or below. If the Mn content is below 1 ppm, Mn can only be detected by spectral analysis. But using higher acceleration energies, the visible lower limit of Mn^{2+} -activated CL could be lower than 4 ppm and possibly lower than 1 ppm. As the scientific relevance of a visible detection limit of CL emission is in question, the spectroscopic detection limit has to be optimized much more in the future. Here will be a high potential using CL spectroscopy to analyze low trace element concentrations in minerals.



Fig. 5. CL photographs. (a) Hydrothermal calcite cement in a pore of a Triassic limestone (Hydra/Greece) showing violet CL if the Mn content is in the range of 12 to 20 ppm (sample K-SUR analyses 1 + 2). (b) Hydrothermal calcite cement sequence showing dark blue and violet colours (sample DB142). In the violet zones (arrow; analyses 3 + 4) Mn and Dy content is in the range of ~3 to ~10 ppm. As violet can be dominantly attributed to Mn^{2+} -activated CL (see Fig. 3a, b), Mn^{2+} -activation is visible although the Mn content is below 10 ppm. (c) Belemnite rostrum (sample OPI analyses 19 + 21). (d) Pleistocene brachiopod shell (sample KAPHIRO, Korinth, Greece) showing blue-violet CL attributed to Mn^{2+} -activation in the range of 4 ppm Mn (1); there violet CL is correlated to ~8 ppm Mn (23).

Obviously, the lower limit of spectroscopically detectable, Mn^{2+} -activated, CL is well below 1 ppm. Here, the linear correlation between CL intensity and the Mn content is the circumstantial evidence that the Mn^{2+} -activation begins in the sub-ppm range. There is in fact no concentration limit for Mn^{2+} -activation in the range of 10–100 ppm Mn content published by numerous authors (e.g. Pierson, 1981; Grover and Read, 1983). There is no reason

why Mn^{2+} -activation could not start at one atom of the irradiated crystal lattice volume if Fe-concentration is low. Thus, the term 'not activated' has to be used carefully if Mn is analyzed and the Fe-content is not high.

There is also a continuous linear increase in Mn^{2+} -activated CL intensity with increasing Mn content, if not sensitized or quenched. This is the circumstantial evidence that CL intensity is initially

dominantly controlled by the absolute Mn concentration. Only at high Mn (>1000 ppm) and Fe content (>3000 ppm) are quenching effects important (Habermann, 1997). Here, selfquenching is more efficient than quenching by Fe^{2+} . But the efficiency of Fe^{2+} -attributed quenching increases with higher Mn concentration (Mason, 1987; Habermann, 1997) which makes quantitative CL spectroscopy still more complicated. The effect of sensitizing by cations like Pb^{2+} needs more attention in future. However, sensitizer elements such as Pb^{2+} most likely have no, or only small, influence on the luminescence intensity if stimulated by an electron beam. It has to be pointed out that sensitizer elements play an important role in photoluminescence investigations (e.g. Gies, 1976; Marfunin, 1979; Kempe et al., 1991).

The experimental data of the linear relationship between Mn content and CL intensity is not consistent with data generated by Savard et al. (1995) where a field of 'erratic' luminescence behaviour is described in the range between ~20 and 200 ppm Mn (analyzed by SIMS and visible CL-intensity determination). As in this range of Mn-content a high conformity of PIXE- and QHRS-CL analyses occurs, these discrepancies presumably are based on the subjective error of a visible detection (see also Hemming et al., 1989). It is clear that a visible determination of the CL intensity is not objectively scientific; it is still 'erratic'. The conclusion is, that if not quenched, the Mn^{2+} -activated luminescence will start at one atom of an irradiated crystal volume. In the case of absent quencher effects the detection of Mn^{2+} -activation at very low concentrations is only limited by the sensibility of the detection system.

Intrinsic luminescence is used to determine non-altered biogenic brachiopods in sediments. However, visible Mn^{2+} -activated CL in recent brachiopods (Barbin and Gaspard, 1995) and their incorporation of Mn in sufficient quantities suggested that fossil brachiopods are not necessarily altered if Mn^{2+} -activated CL is present. Additionally, Barbin and Gaspard (1995) pointed out that zones of intrinsic ('non-luminescent') and Mn^{2+} -activated calcite of brachiopods may correspond to particular periods and/or environmental conditions during life of the organisms. Such evidence must to be considered in future studies, especially when using CL to select brachiopods for isotopic studies. The same applies to

the use of belemnites. Moreover, we think it will be of priority to study the CL properties and structure of modern biogenic calcite first, before using CL to estimate the diagenetic alteration of fossil brachiopod shells and belemnites. In this field the work of Barbin and Gaspard (1995) is instructive. However, the intrinsic CL of calcite is based on lattice defects like for example electron or oxygen vacancies and broken metal-ion oxygen bondings. As these defects are not merely confined to biogenic calcite, defining unaltered biogenic calcite by their intrinsic CL is no unequivocal criterion. CL is a powerful and very sensitive method, and for that reason it has to be used knowing not only its analytical potential but also its limitations.

Acknowledgements

We would like to thank Bruce Sellwood for the constructive review. The investigations were supported by grants of the German Science Foundation (DFG Ri 216-13/1-2).

References

- Amieux, P., 1982. La cathodoluminescence: méthode d'étude sédimentologique des carbonates. Bull. Cent. Rech. Explor. Prod. Elf-Aquitaine 6, 437–483.
- Barbin, V., Gaspard, D., 1995. Cathodoluminescence of recent articulate brachiopod shells. Implications for growth stages and diagenesis evaluation. *Geobios* 26 (6), 701–710.
- Bruhn, F., 1995. Kombinierte Spurenelement-Mikroanalysen und Kathodolumineszenz-Untersuchungen: Entwicklung einer Meßmethodik für die Bochumer Protonenmikrosonde (PIXE) und Fallstudien aus der Sedimentologie. Diss., Ruhr-Universität, Bochum, 172 pp.
- Calderón, T., Aguilar, M., Jaque, F., Coy-Yll, R., 1984. Thermoluminescence from natural calcite. *J. Phys.* 17: 2077–2038.
- Füchtbauer, H., Richter, D.K., 1988. Karbonate. In: Füchtbauer, H. (Ed.), *Sedimentpetrologie, Teil II. Sedimente und Sedimentgesteine*. Schweizerbart, Stuttgart, pp. 233–434.
- Gies, H., 1976. Zur Beziehung zwischen Photolumineszenz und Chemismus natürlicher Karbonate. *Neues Jahrb. Mineral. Abh.* 172, 1–46.
- Grover, J.R., Read, J.F., 1983. Paleoaquifer and deep burial related cements defined by regional cathodoluminescence pattern, Middle Ordovician carbonates, Virginia. *Am. Assoc. Pet. Geol. Bull.* 67, 1275–1303.
- Habermann, D., 1997. Quantitative hochauflösende Kathodolumineszenz-Spektroskopie von Calcit und Dolomit. Diss., Ruhr-Universität, Bochum, 152 pp.
- Habermann, D., Neuser, R.D., Richter, D.K., 1996a. REE-acti-

- vated cathodoluminescence of calcite and dolomite: High Resolution Spectrometric analysis of CL emission (HRS-CL). *Sediment. Geol.* 101, 1–7.
- Habermann, D., Neuser, R.D., Richter, D.K., 1996b. Quantitative high resolution spectral analysis of Mn^{2+} in sedimentary calcite. *Int. Conf. Cathodoluminescence and Related Techniques in Geoscience and Geomaterial*, Nancy, Abstr. pp. 65–66.
- Hemming, N.G., Meyers, W.J., Grams, J.C., 1989. Cathodoluminescence in diagenetic calcites: The role of Fe and Mn as deduced from electron probe and spectrophotometric measurements. *J. Sed. Petrol.* 59, 404–411.
- Honman, N.P.O., Yang, C., Malmqvist, K.G., 1994. A highly sensitive method for rare-earth element analysis using ionoluminescence combined with PIXE. *Nucl. Instr. Methods Phys. Res.* A353, 610–614.
- Johansson, S.A.E., Campbell, J.L., 1988. *PIXE: A Novel Technique for Elemental Analysis*. Wiley, Chichester, 347 pp.
- Kempe, U., Trinkler, M., Wolf, D., 1991. Yttrium und Seltenerd-fotolumineszenz natürlicher Scheelite. *Chem. Erde* 51, 275–289.
- Land, L.S., 1995. Comment on 'Oxygen and carbon isotopic composition of Ordovician brachiopods: implications for coeval seawater' by H. Qing and J. Veizer. *Geochim. Cosmochim. Acta* 59, 2843–2844.
- Machel, H.G., Mason, R.A., Mariano, A.N., Mucci, A., 1991. Causes and emission of luminescence in calcite and dolomite. In: Barker, C.E., Kopp, O.C. (Eds.), *Luminescence Microscopy and Spectroscopy: Qualitative and Quantitative Applications*. SEPM Short Course 25, 9–25.
- Marfunin, A.S., 1979. *Spectroscopy, Luminescence and Radiation Centres in Minerals*. Translated from Russian by V.V. Schiffer, Springer-Verlag, Berlin, 352 pp.
- Mason, R.A., 1987. Ion microprobe analysis of trace elements in calcite with an application to the cathodoluminescence zonation of limestone cements from the Lower Carboniferous of South Wales, U.K. *Chem. Geol.* 64, 209–224.
- Mason, R.A., Mariano, A.N., 1990. Cathodoluminescence activation in manganese bearing and rare-earth bearing synthetic calcites. *Chem. Geol.* 88, 191–206.
- Meijer, J., Stephan, A., Adamczewski, J., Bukow, H.H., Rolfs, C., Pickart, T., Bruhn, F., Veizer, J., 1994. PIXE microprobe for geoscience applications. *Nucl. Instr. Meth.* B89, 229–232.
- Neuser, R.D., 1995. A new high-intensity cathodoluminescence microscope and its application to weakly luminescing minerals. *Bochumer Geol. Geotech. Arb.* 44, 116–118.
- Neuser, R.D., Bruhn, F., Götze, J., Habermann, D., Richter, D.K., 1996. Kathodolumineszenz: Methodik und Anwendung. *Zbl. Geol. Paläontol. Teil 1*, 1995 (1/2), 287–306.
- Pierson, J.R., 1981. The control of cathodoluminescence in dolomite by iron and manganese. *Sedimentology* 28, 331–336.
- Qing, H., Veizer, J., 1994. Oxygen and carbon isotopic composition of Ordovician brachiopods: implication for coeval seawater. *Geochim. Cosmochim. Acta* 58, 4429–4442.
- Richter, D.K., Zinkernagel, U., 1981. Zur Anwendung der Kathodolumineszenz in der Karbonatpetrographie. *Geol. Rundsch.* 70, 1276–1302.
- Savard, M.M., Veizer, J., Hinton, R., 1995. Cathodoluminescence at low Fe and Mn concentrations: a SIMS study of zones in natural calcites. *J. Sediment. Res.* A65, 208–213.
- Sippel, R.F., Glover, E.D., 1965. Structures in carbonate rocks made visible by luminescence petrography. *Science* 150, 1283–1287.
- Ten Have, T., Heijnen, W., 1985. Cathodoluminescence activation and zonation in carbonate rocks: an experimental approach. *Geol. Mijnbouw* 64, 297–310.
- Walker, G., Abumere, O.E., Kamaluddin, B., 1989. Luminescence spectroscopy of Mn^{2+} centers in rock-forming carbonates. *Mineral. Mag.* 53, 201–211.